Electrode Biasing Experiment in the Large Helical Device

S. Kitajima 1), H. Takahashi 2), K. Ishii 1), J. Sato 1), T. Ambo 1), M. Kanno 1), A. Okamoto 1), M. Sasao 1), S. Inagaki 3), M. Takayama 4), S. Masuzaki 2), M. Shoji 2), N. Ashikawa 2), M. Tokitani 2), M. Yokoyama 2), Y. Suzuki 2), T. Shimozuma 2), T. Ido 2), A. Shimizu 2), Y. Nagayama 2), T. Tokuzawa 2), K. Nishimura 2), T. Morisaki 2), S. Kubo 2), H. Kasahara 2), T. Mutoh 2), H. Yamada 2), Y. Tatematsu 5) and LHD experimental group

1) Department of Quantum Science and Energy Engineering, Tohoku University, Sendai, Japan
2) National Institute for Fusion Science, Toki, Japan
3) Kyushu University, Hakozaki, Fukuoka, Japan
4) Akita Prefectural University, Honjyo, Akita, Japan
5) University of Fukui, Fukui, Japan

E-mail contact of main author: sumio.kitajima@qse.tohoku.ac.jp

Abstract. The transition to the improved confinement mode by the electrode biasing was observed for the first time in the Large Helical Device (LHD). The negative resistance was observed in the confinement mode sustained by the cold electrode biasing. The electrode current showed the clear decrease against to the increase in the electrode voltage and had hysteresis in the transition phenomena. The decrease in the electrode current suggested the improvement of the radial particle transport. The increase in the energy confinement time and remarkable suppression of the density fluctuation, which correspond to the transition, were also observed. These results indicated that the electrode biased plasma in LHD showed the similar improvements in confinement to the observations in the H-mode plasma in tokamaks and stellarators.

1. Introduction

In neoclassical theories the nonlinearity of the ion viscosity plays the important role in the bifurcation phenomena of the L-H transition [1-6], which observed in tokamaks and stellarators [7-11]. The effects of the ion viscosity maxima on the transition to an improved confinement mode were experimentally investigated by the externally controlled $\boldsymbol{J} \times \boldsymbol{B}$ driving force for a poloidal rotation using the hot cathode biasing in Tohoku University Heliac (TU-Heliac) [12-20]. Here, $\boldsymbol{J}$ and $\boldsymbol{B}$ are a biasing electrode current and a magnetic field. In steady state the external $\boldsymbol{J} \times \boldsymbol{B}$ driving force balances with the ion viscous damping force and the friction to neutral particles. Then the ion viscosity opposing to the poloidal rotation can be estimated experimentally by subtracting the friction term from the driving force [19]. Therefore it is important to verify whether the transition phenomena observed in TU-Heliac can appear in the wide plasma parameter range and in the confine systems that have different magnetic configuration. The importance of the biasing experiment in stellarators exists in the ability to understand universally the relation between the transition behaviour and the viscosity by taking high order magnetic Fourier components into viscosity evaluation. The optimization of helical ripples allows the reduction of viscosity, which is expected to bring good accessibilities to the improved confinement modes. In this paper we report the electrode biasing experiments in LHD, which had the different toroidicity and helicity (m/n=1/1 in Heliac, 2/-1 in CHS, LHD) and can produce the low collisional plasma.

2. Biasing experiments in CHS

We tried the hot cathode biasing on CHS in the low field and the low temperature Argon plasma ($n_e \sim 0.5\times10^{18}$ m^{-3}, $T_e \sim 8$ eV and $B_0 \sim 0.09$ T) using the electrode current scanning

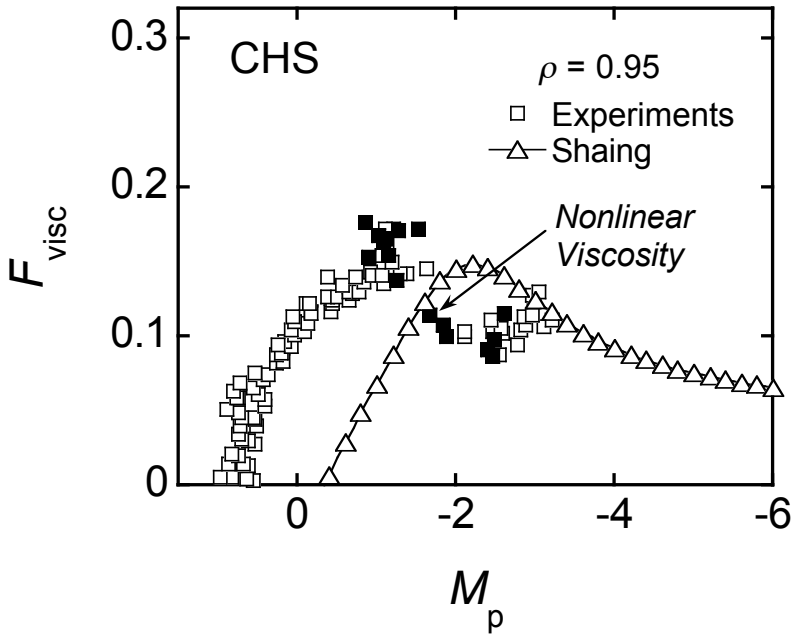

FIG. 1 Relation between the normalized viscosities and poloidal Mach number M_p in CHS

same method as TU-Heliac [19]. The target plasma for the biasing was produced by ECH (f = 2.45 GHz, P_{out} ~ 40 kW). We observed the transition accompanied with a negative resistance, the suppression of ion density fluctuation and the increase in the stored energy. Here the negative resistance means that the decrease in the electrode current with increasing the electrode voltage. We evaluated the relation between the normalized ion viscosity F_{visc} and

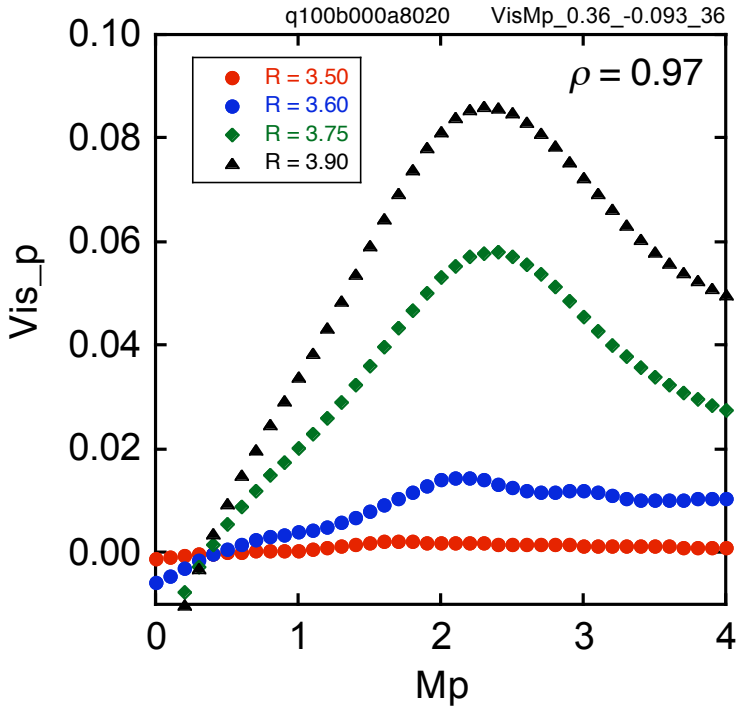

FIG. 2 Relation between the normalized viscosity V_{vis_p} and poloidal Mach number M_p in LHD

the poloidal Mach number M_p as shown Fig. 1. The electron density, temperature and the space potential were measured by a Langmuir probe. The ion viscosity has local maximum and the dependence of ion viscosity on M_p qualitatively agreed with the neo-classical model [4] and the transition appeared when the external driving force exceeded a local maximum in the viscosity. We also revealed that the relation between the electrode voltage and current had negative resistance characteristics in the region where the viscosity had the non-linearity (denoted by the closed rectangle symbol in Fig. 1).

Therefore it is important to continue the biasing experiment in a high-performance plasma, namely, low collisional plasma in LHD. The calculated ion viscosities at $\rho = 0.97$ in LHD by the neoclassical theory [4] are shown in Fig.2 in various configurations (R_{ax} = 3.50, 3.60, 3.75 and 3.90 m, here R_{ax} is the major radius of the magnetic axis). Figure 2 clearly shows that the local maxima in the ion viscosity drastically change depending on the magnetic axis position in LHD.

3. Biasing experiments in LHD

The target magnetic configuration in LHD for the electrode biasing was selected the configuration of R_{ax} = 3.60 m in Fig. 2 and a toroidal magnetic field B_t = 2.75 T. The target plasma for the biasing was produced by ECH (f = 77 GHz, P_{out} ~ 0.2 MW). The electron density and temperature at the magnetic axis were ~ 8×10^{18} m^{-3} and ~ 0.8 keV in the Helium target plasma which had the sufficiently low collisionality to neutral particles to ignore the friction effect.

3.1. Experimental setup

We designed the electrode biasing system for a high-temperature and high-density plasma in a large device. The shape of the electrode was a cylindrical disk of diameter 100 mm and length 40 mm and the material of the electrode was Carbon as shown in Fig.3. The residual gas in the electrode was removed by a baking before install. The electrode was connected to the support shaft made of SUS316, which was electrically isolated from the Carbon disk and covered by a Boron Nitride pipe in order to insulate the electrode from the grand potential. Then the electrode can be inserted into the plasma avoiding a short circuit between the inside and the outside of the separatrix. The connection part for the feed lines of the electrode and the connection part to the driving system were also covered with Carbon in order to protect from the plasma in the scrape-off layer as shown in Fig.3. All part shown in Fig.3 was connected to the linear driving system and inserted to the plasma from the under port in LHD. The electrode temperature measured by an IR camera increased up to 400°C after about 30 shots in the biasing experiment.

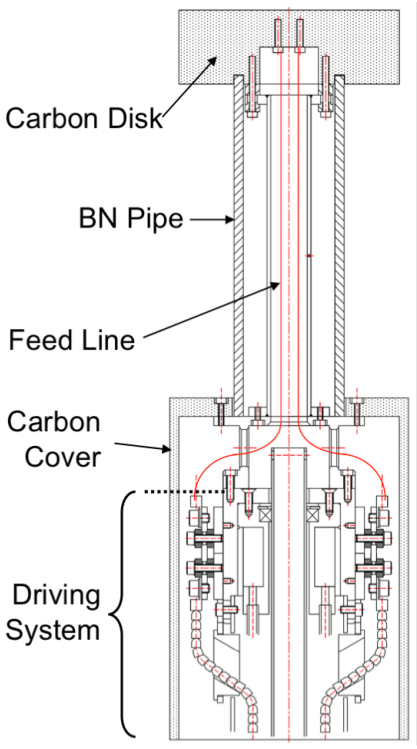

FIG. 3 Carbon electrode and supporting system

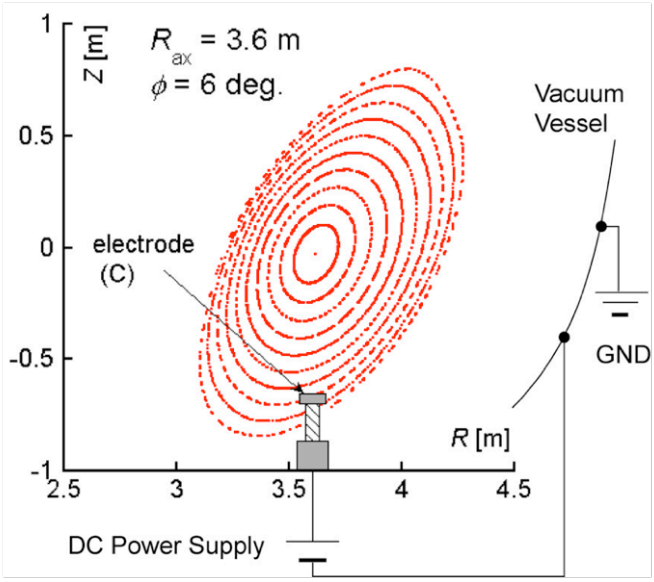

FIG. 4 Flux surfaces and Carbon electrode. Electrode was positively biased against to the vacuum vessel.

The relation between flux surfaces in the configuration of R_{ax} = 3.60 m and the Carbon electrode were shown in Fig. 4. In the biasing experiment the centre of the electrode was inserted to $\rho \sim 0.8$. The electrode was connected to the vacuum vessel through the DC power supply (V_{out} = 650V max, I_{out} = 46A max), which had cc and cv operation mode. In this experiment the electrode was positively biased against to the vacuum vessel.

3. 2. Experimental results in LHD

The target plasma for the biasing in LHD was produced by ECH in the magnetic configuration (R_{ax} = 3.60 m, B_t = 2.75 T). The electron density and temperature at the magnetic axis were ~ 8×10^{18} m^{-3} and ~ 0.8 keV in the Helium target plasma.

Figure 5 shows the typical time evolutions of (a) the electrode voltage V_E, (b) the electrode current I_E, (c) the averaged electron density n_e along the chord passing through the magnetic axis measured by an FIR interferometer and (d) the energy confinement time estimated from $W_p /(P_{ECH} + I_E V_E - dW_p/dt)$, here W_p was a stored energy.

The ECH (f = 77 GHz, $P_{out} \sim 0.2$ MW) was applied from t = 0.21 s to t = 1.21 s (hatched region in Fig. 5). The electrode was positively biased through the power supply, thus collecting electrons. In order to change the external $\boldsymbol{J} \times \boldsymbol{B}$ driving force linearly we adopted the triangle input waveform for the power supply. A ramp-up interval is the time from t = 0.9 s to t = 1.0 s and a ramp-down is the time from t = 1.0 s to t = 1.1 s as shown Fig. 5(a). In the ramp down electrode voltage case the electrode voltage did not follow in the input waveform because of the characteristics of the power supply. The output voltage remained because of a high impedance load for the power supply.

Figure 5(b) shows the sudden current drops (0.99 s < t < 1.06 s) in the electrode current, which means the negative resistance and suggested the transition to another confinement mode. Figure 6 shows the relation between the electrode voltage and the electrode current. We also tried to bias the electrode with the fixed voltage before the ramp-up and ramp-down biasing. The rectangle symbols in Fig. 6 show the fixed voltage biasing cases in which the electrode was biased by the rectangle waveform. In this case the electrode characteristics also shows the negative resistance, however the fixed voltage biasing was not convenient for the survey of transition points. Therefore we adopted the triangle waveform for the biasing shown in Fig. 5(a). The solid line shows the triangle waveform case. It clearly shows the transition points and the negative resistance characteristics, which suggests the improvement of the radial particle transport. The electrode voltage at the forward transition (V_E ~ 470 V) was greater than that at the reverse transition (V_E ~ 430 V). Therefore the electrode characteristics had the *hysteresis* in the transition phenomenon.

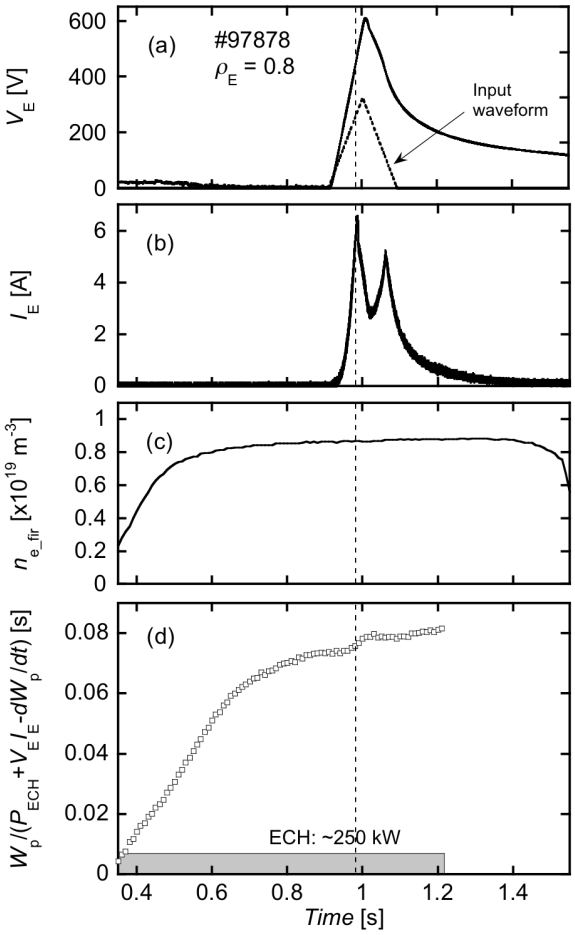

FIG. 5 Typical time evolutions of (a) the electrode voltage V_E, (b) the electrode current I_E, (c) the averaged electron density n_e at the magnetic axis and (d) the confinement time

The energy confinement time was estimated taking the input power of the biasing into account. Then, the energy confinement time τ_E was estimated from the following relation

$$\frac{dW_p}{dt} = P_{ECH} + I_E V_E - \frac{W_p}{\tau_E} \qquad (1)$$

where W_p, P_{ECH}, I_E and V_E are a stored energy, an ECH output power, an electrode current and an electrode voltage respectively. The stored energy W_p was measured by the diamagnetic loop. In Fig. 5(d) the energy confinement time τ_E increased about 8 % correspond to the transition, which suggests the consistency with the improvement of the radial particle transport (the negative resistance characteristics in the electrode current in the region 0.99 s < t < 1.06 s). However the significant changes in the averaged electron density n_e along the chord passing through the magnetic axis was not clearly seen in Fig. 5 (c).

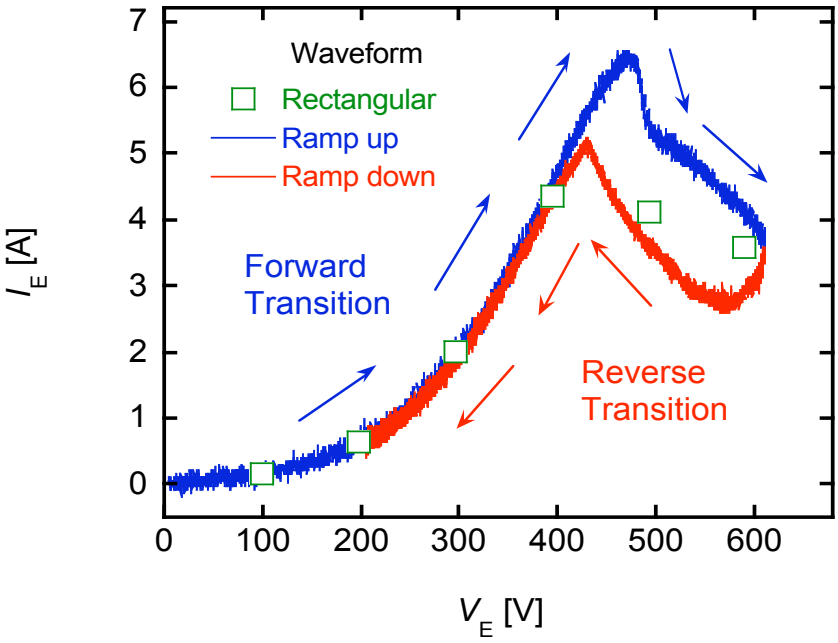

FIG. 6 Relation between the electrode voltage V_E and the electrode current I_E

3. 3. Fluctuation measurement

We also measured the density fluctuation by the microwave reflectometers (f = 65 GHz), which were set at the toroidal angles separated from the electrode by 18°and 162° in the toroidal direction. Figure 7 shows the power spectrum of the density fluctuation at $\rho \sim 0.8$ measured by the microwave reflectometers at the toroidal angles separated from the electrode

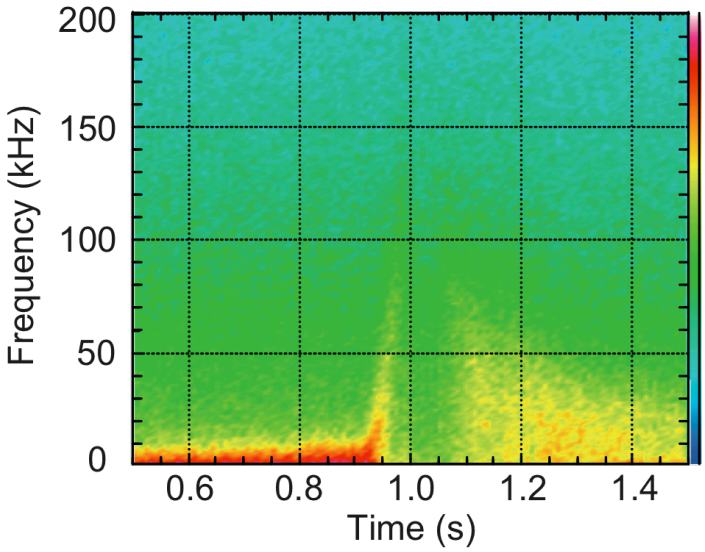

FIG. 7 Power spectrum of the density fluctuation measured by the microwave reflectometer separated from the electrode by 18°

by 18°. Figure 7 reveals the remarkable suppression of the density fluctuation in wide frequency range correspond to the transition in the region 0.99 s < t < 1.06 s. The suppression in the density fluctuation coincide with the negative resistance characteristics in the electrode current and the increase in the energy confinement, which suggests that the increase in the energy confinement time relates to the suppression density fluctuation. These observations indicate that the electrode biasing in TU-Heliac, CHS and LHD successfully triggered the transition phenomena, which have different magnetic topology.

4. Summary

We designed the electrode biasing system for a high-temperature and high-density plasma in a large device and successfully and safely performed the biasing experiments in the low collisional plasma in LHD. We observed the negative resistance in the electrode characteristics in the confinement mode sustained by the cold electrode biasing. The electrode current showed the clear decrease against to the increase in the electrode voltage and had hysteresis in the transition phenomena. The decrease in the electrode current suggested the improvement of the radial particle transport. We also observed the increase in the energy confinement time and remarkable suppression of the density fluctuation, which correspond to the transition. These results indicated that the electrode biased plasma in LHD showed the similar improvements in confinement to the observations in the H-mode plasma in tokamaks and stellarators and also indicate that the electrode biasing in TU-Heliac, CHS and LHD successfully triggered the transition phenomena, which have different magnetic topology.

Acknowledgments

This work was supported by the LHD Joint Planning Research programme at the National Institute for Fusion Science.

References

[1] ITOH, S.-I., ITOH, K., Phys Rev. Lett. **60** (1988) 2276.
[2] SHAING, K. C., CRUME, J. E. C., Jr., Phys Rev. Lett. **63** (1989) 2369.
[3] SHAING, K. C., Phys Fluids B **5** (1993) 3841.
[4] SHAING, K. C. Phys Rev. Lett. **76**, 4364 (1996).
[5] ROZHANSKY, V., TENDLER, M., Phys. Fluids B **4** (1992) 1877.
[6] CORNELIS, J. *et al.*, Nucl. Fusion **34** (1994) 171.
[7] WAGNER, F. *et al.*, Phys. Rev. Lett. **49** (1982) 1408.
[8] BURRELL, K. H. *et al.*, Phys. Rev. Lett. **59** (1987) 1432.
[9] KOTSCHENREUTHER, M. *et al.*, Phys. Plasmas **2** (1995) 2381.
[10] ERCKMANN, V. *et al.*, Phys. Rev. Lett **70** (1993) 2086.
[11] TOI, K. *et al.*, Plasma Phys. Control. Fusion **38** (1996) 1289.
[12] KITAJIMA, S. *et al.*, Jpn. J. Appl. Phys. **30** (1991) 2606.
[13] INAGAKI, S. *et al.*, Jpn. J. Appl. Phys. **36** (1997) 3697.
[14] KITAJIMA, S. *et al.*, J. of Plasma and Fusion Research SERIES **4** (2001) 391.
[15] KITAJIMA, S. *et al.*, Int. J. Appl. Electromagnetics and Mechanics **13** (2002) 381.
[16] TAKAHASHI, H., KITAJIMA, S. *et al.*, J. of Plasma and Fusion Research SERIES **6** (2003) 366.
[17] TANAKA, Y., KITAJIMA, S. *et al.*, J. of Plasma and Fusion Research SERIES **6** (2003) 371.

[18] TAKAHASHI, H. *et al*., Plasma Phys. Control. Fusion **48** (2006) 39.
[19] KITAJIMA, S. *et al*., Nucl. Fusion **46** (2006) 200.
[20] KITAJIMA, S. *et al*., Nucl. Fusion **48** (2008) 035002.